Microcontroller Implementation of Current Modulated Edge Emitting Semiconductor Lasers with Pulse Packages and Chimera States in Its Network

Dhanagopal Ramachandran
Chennai Institute of Technology
Nasr Saeed
University of Nyala
André Rodrigue Tchamda
University of Dschang: Universite de Dschang
Sifeu Takougang Kingni (stkingni@gmail.com)
University of Maroua: Universite de Maroua
Anitha Karthikeyan
Chennai Institute of Technology
Iqtadar Hussain
Qatar University

Research Article

Keywords: Edge emitting semiconductor laser, current modulation, periodic and chaotic pulse packages, microcontroller implementation, coherent and incoherent behavior, chimera states

Posted Date: March 11th, 2022

DOI: https://doi.org/10.21203/rs.3.rs-912617/v1

Microcontroller implementation of current modulated edge emitting semiconductor lasers with pulse packages and chimera states in its network

Dhanagopal Ramachandran[1], Nasr Saeed[2], André Rodrigue Tchamda[3], Sifeu Takougang Kingni[4,*], Anitha Karthikeyan[5] and Iqtadar Hussain[6]

[1] *Center for Systems Design, Chennai Institute of Technology, Chennai-600069, Tamilnadu, India*

[2] *Department of Physics, College of Education, Nyala University, P.O. Box: 155, Nyala, Sudan*

[3] *Department of Rural Engineering, Faculty of Agronomy and Agricultural Sciences, University of Dschang, P.O Box 222, Dschang, Cameroon*

[4] *Department of Mechanical, Petroleum and Gas Engineering, Faculty of Mines and Petroleum Industries, University of Maroua, P.O. Box 46, Maroua, Cameroon*

[5] *Center for Nonlinear Systems, Chennai Institute of Technology, Chennai-600069, Tamilnadu, India*

[6] *Department of Mathematics, Statistics and Physics, Qatar University, Doha 2713, Qatar*

* *Corresponding author: stkingni@gmail.com*

Abstract

This paper investigates the dynamical behavior of a single and a network of current modulated edge emitting semiconductor lasers (CMEESLs). Different dynamical behaviors of CMEESL are revealed in two-dimensional parameters space by varying the amplitude and frequency of modulation. Single CMEESL exhibits periodic pulse packages followed by period-doubling cascade to chaotic pulse packages for frequency of modulation current density less than *1* GHz. Microcontroller results which agree with numerical results of single CMEESL are presented. To investigate the dynamics in a network of CMEESLs, a nonlocally coupled lattice array of CMEESLs is analyzed numerically by varying the coupling strength. It is found that the coupling strength plays a significant role in the coherent and incoherent behaviors of the nodes in the network. For a small range of coupling strength, the network exhibits chimera states which are confirmed by their respective state plots. Synchronization error between the nonlocally coupled CMEESLs is also presented to show the existence of chimera states.

Keywords: Edge emitting semiconductor laser, current modulation, periodic and chaotic pulse packages, microcontroller implementation, coherent and incoherent behavior, chimera states.

I- Introduction

Lasers are used in almost all domains after its first invention **[1]**. Among the different type of lasers, semiconductor lasers are widely available, as it is easily manufactured and tailored by means of the lithographic production process. Due to its availability, it is virtually used in areas such as; high data rate modulated transmitter, optical medical application, neural and metro access networks, optical spectroscopy, optical metrology, optical sensing and random number generation **[2-6]**. The dynamics of semiconductor lasers has interesting applications and has attracted extensive studies. These studies have been done because of the sensitivity of laser medium to external perturbations: Optical feedback, optoelectronic feedback, optical injection and external modulation of the injection current. Usually, these perturbations lead to dynamical instabilities, such as self-pulsation, quasi-periodicity, frequency-locked states, regular or irregular pulse packages and chaos. The instabilities induced in semiconductor lasers by external perturbations can be useful for engineering applications. For example, semiconductor lasers with current modulation are necessary for high-bit speed optical communication systems **[7-12]**.

The dynamics of semiconductor lasers subject to current modulation has been extensively investigated in the literature. Semiconductor ring lasers subject to current modulation exhibit a period-doubling dynamics to in-phase chaos, similar to CMEESL at modulation frequency of the same order or higher than the relaxation oscillations frequency. While at lower modulation frequency, the counter-propagating modes of semiconductor ring lasers displayed period doubling transition in anti-phase chaotic regime without the involvement of any carrier dynamics **[13]**. Vertical cavity surface-emitting lasers (VCSELs) subject to current modulation emit single pulse or package of pulses for a couple of hundreds MHz of modulation frequency and for few GHz of modulation frequency. The polarization modes of VCSELs exhibit a period-doubling transition to chaotic behavior **[14–18]**. In **[19]**, Chembo and Woafo performed the stability analysis for the synchronization of ultra-high frequency CMEESLs both in their periodic and chaotic regimes. They demonstrated numerically that CMEESL exhibits periodic-1-oscillations, periodic doubling cascade and lastly chaotic behaviors for ultra-high frequency current modulation.

This paper based on numerical and electronic implementations generates periodic (regular) and chaotic (irregular) pulse packages in single CMEESL with frequency of current modulation less than *1* GHz and investigates the network dynamics of CMEESLs, in which individual subsystems are characterized by chaotic pulse packages. After the first demonstration of regular pulse packages in edge emitting semiconductor laser with short time delay optical feedback **[20]**, regular and irregular pulse packages have also been observed in VCSELs with short time delay optical feedback **[21]**. In **[22]**, the authors experimentally observed pulse package oscillations in broad area semiconductor laser with short optical feedback for relatively strong optical feedback, with a lower bias injection current close to the threshold. Regular pulse packages have also been found in VCSELs with low frequency of current modulation **[17, 18]**.

The paper is organized as follow: Section 2 presents the dynamical analysis and microcontroller implementation of single CMEESL, section 3 deals with the collective behavior in CMEESL network. Finally, the conclusion is given in section 4.

II- Dynamical analysis and microcontroller implementation of single CMEESL

The single-mode-rate equations showing the relation between photon density P' and carrier density N can be used to describe the dynamical of single CMEESL **[19]**. The mathematical equations are given as follows:

$$\frac{dP'}{dt'} = \left[g\left(N - N_0\right)\left(1 - sP'\right) - \frac{1}{\tau_p} \right] P', \tag{1a}$$

$$\frac{dN}{dt'} = I\left(t'\right) - \frac{N}{\tau_s} - g\left(N - N_0\right)\left(1 - sP'\right) P', \tag{1b}$$

where t' is the time, s is the nonlinear gain suppression factor, and g is the gain coefficient. The parametrs τ_s and τ_p are the carrier and photon lifetimes, and N_0 is the carrier density required for transparency. The parameter $I\left(t'\right)$ is the injection current density modulated according to $I\left(t'\right) = I_{dc} + I_m \sin\left(2\pi f_m t'\right)$, where I_{dc} is the dc bias current density, I_m is the amplitude of the

modulation, and f_m is the modulation frequency. A suitable normalization of equations (1a)–(1b) leads to the following dimensionless form:

$$\frac{dP}{dt} = \left[\left(1+2n\right)\left(1-\sigma P\right)-1\right]P, \tag{2a}$$

$$\frac{dn}{dt} = \varepsilon_0 \left\{ i_{dc}\left[1+m\sin\left(\omega t\right)\right] - n - \left(1+2n\right)\left(1-\sigma P\right)P \right\}, \tag{2b}$$

with the following rescaling :

$$t = \frac{t'}{\tau_p},\ \varepsilon_0 = \frac{\tau_p}{\tau_s},\ \sigma = \frac{2s}{g\,\tau_s},\ P = \left(\frac{g\tau_s}{2}\right)P',\ g\left(N_{th}-N_0\right) = \frac{1}{\tau_p},\ n = \frac{1}{2}g\tau_p\left(\frac{N}{N_{th}}-1\right),\ I_{th} = \frac{N_{th}}{\tau_s}, \tag{3}$$

$$i_{dc} = \frac{I_{dc}-I_{th}}{I_{th}},\ m = \frac{I_m}{I_{dc}-I_{th}},\ \omega = 2\pi f_m \tau_p,$$

where I_{th} is the threshold injection current density, and N_{th} is the threshold carrier density. The numerical values of the parameters are identical to those of **[19]**: $g = 8.4\times10^{-13}\,m^3\,s^{-1}$, $s = 5.0\times10^{-27}\,m^3$, $N_{th} = 2.018\times10^{24}\,m^{-3}$, $N_0 = 1.435\times10^{24}\,m^{-3}$, $\tau_s = 1.025\,ns$, $\tau_p = 2.041\,ps$ and $I_{th} = 1.969\times10^{33}\,m^{-3}\,s^{-1}$.

The dynamical behaviors of single CMEESL versus the modulation parameters m and f_m for specific value of parameter i_{dc} are plotted in Fig. 1.

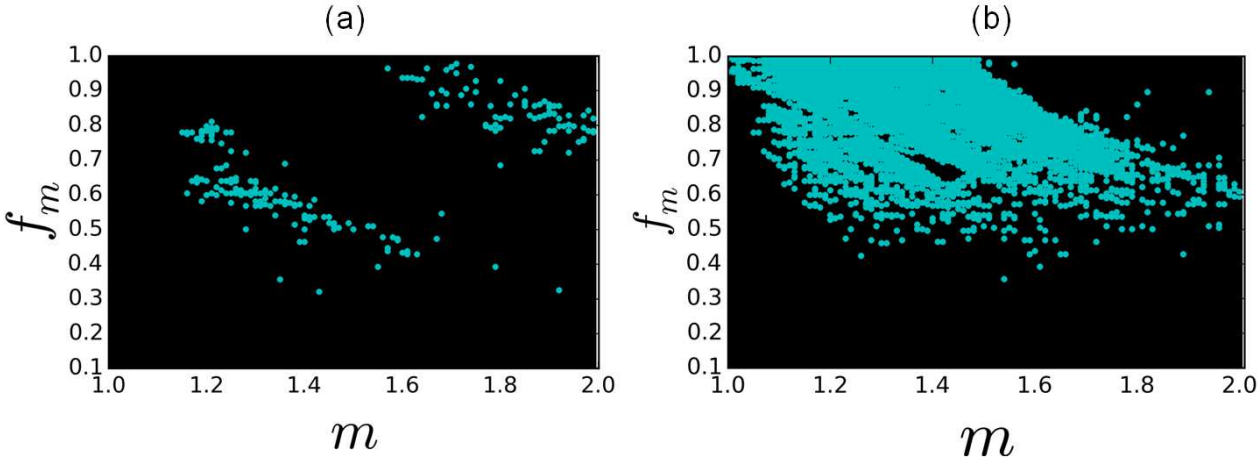

Figure 1: Different dynamical behaviors in the $\left(m,\ f_m\left[GHz\right]\right)$ parameter space for specific value of parameter i_{dc} : (a) $i_{dc} = 0.1$ and (b) $i_{dc} = 0.6$.

In Figure 1, black color represents periodic behaviors while cyan color indicates the chaotic behaviors. The increase of parameter i_{dc} leads to a wider range of chaotic behavior all over the

parameter space in Fig. 1 (b) compared to Fig. 1 (a). For $i_{dc} = 0.6$ and $m = 1.1$, bifurcation diagram of photon density *P* and corresponding largest Lyapunov exponent (LLE) versus frequency of modulation f_m are plotted in Fig. 2.

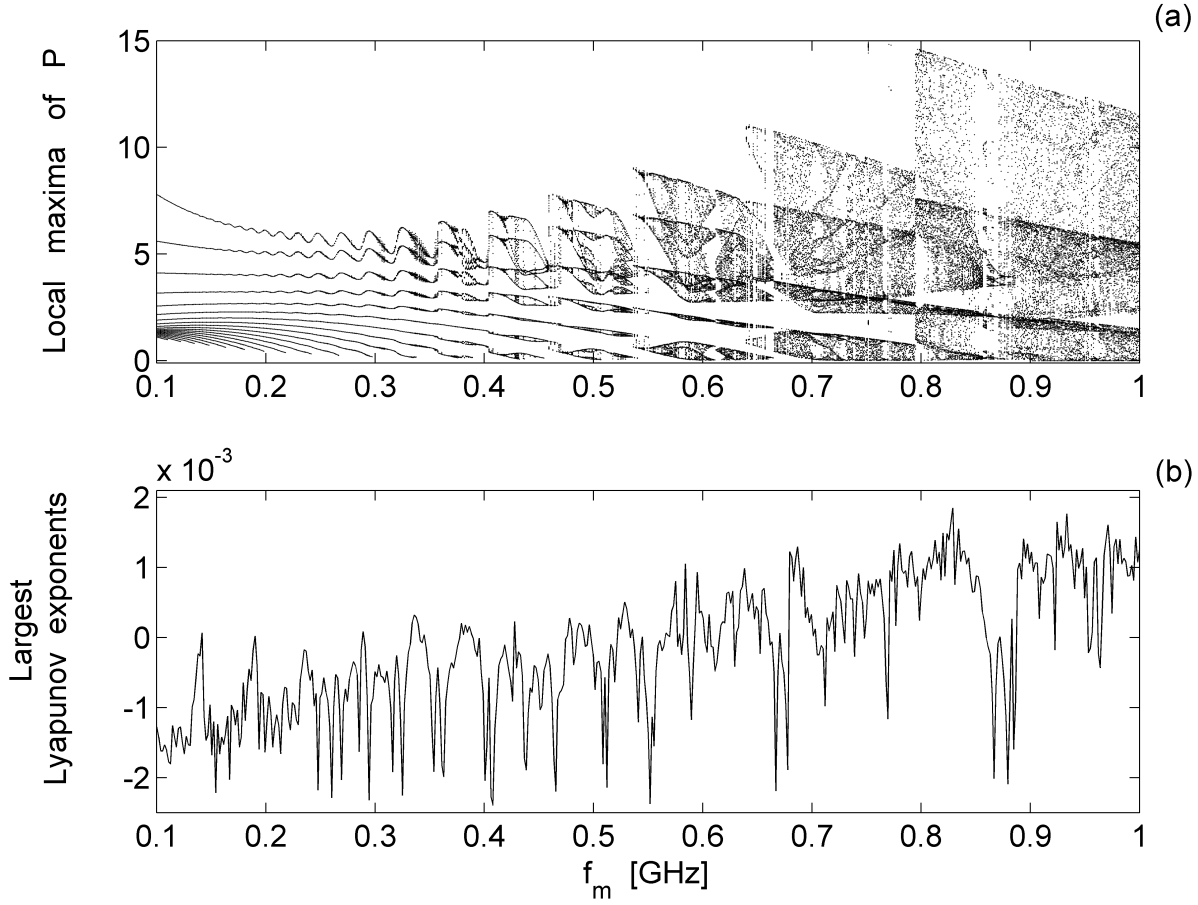

Figure 2: Bifurcation diagram depicting local maxima of P (a) and corresponding LLE (b) versus frequency of modulation f_m for $i_{dc} = 0.6$ and $m = 1.1$.

When the frequency of modulation varies from *0.1* to *1* GHz, single CMEESL displays periodic behaviors through period-doubling cascade to chaotic behaviors. The dynamical behaviors observed in Fig. 2 (a) are confirmed by the LLE of Fig. 2 (b). The dynamical behaviors depicted in Fig. 2 are further detailed in Figs. 3 and 4, which show the time histories of P, n, $i(t) = i_{dc}\left[1 + m\sin(\omega t)\right]$ and phase plane for specific values of frequency of modulation f_m.

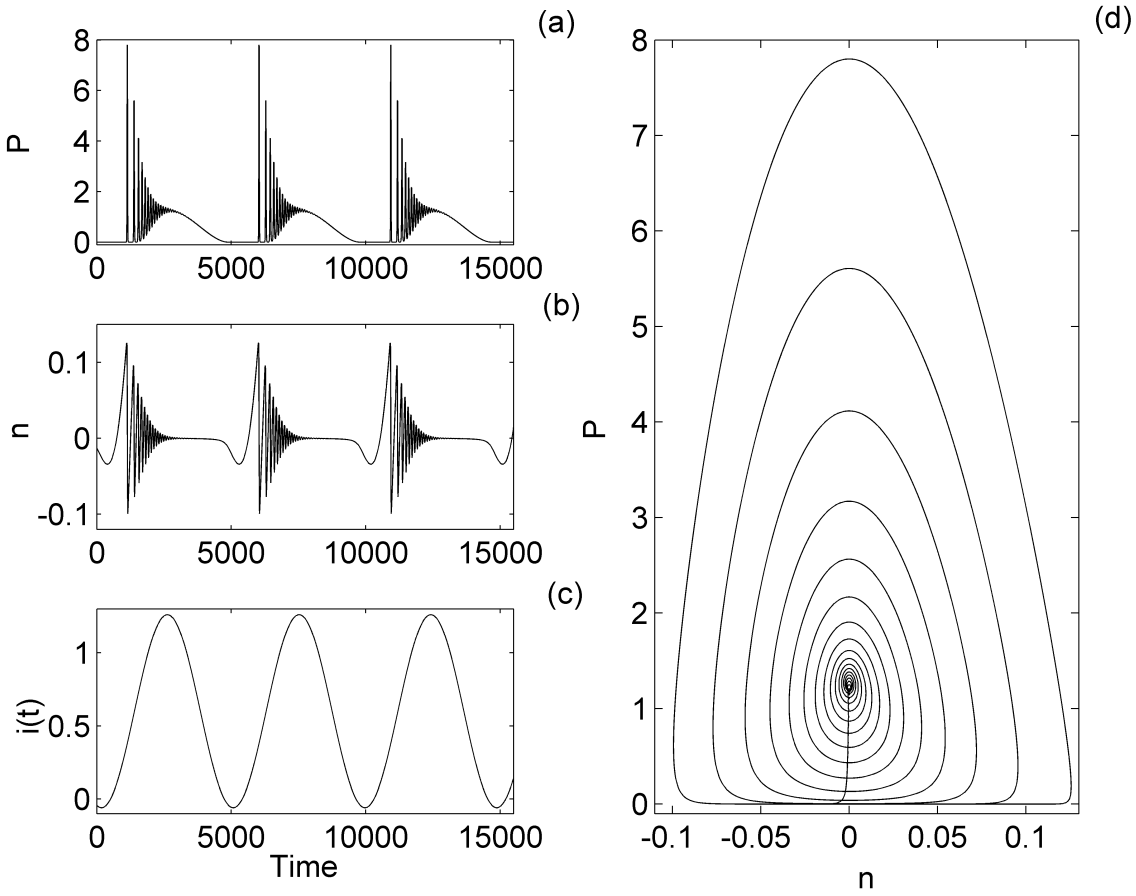

Figure 3: Time histories of P, n, $i(t)$ and phase plane for $f_m = 100\ MHz$. The others parameters are $i_{dc} = 0.6$ and $m = 1.1$. The initial conditions are ($P(0)$, $n(0)$) = (0.1, 0.001).

The photon density P and the carrier density n generate a sequence of pulses with decreasing amplitude for $f_m = 100\ MHz$ as shown in Figs. 3 (a) and (b), respectively. These pulses are assembled in package. All packages have the same shape and appear regularly at the frequency of modulation. Each package is made of regular spaced pulses and it is separated to its direct neighbour by oscillations with very small amplitude. The photon density P and carrier density n describe the dynamics of relatively fast changing processes while the injection current $i(t)$ describes the relatively slowly changing quantity which modulates the photon density P and carrier density n (see Fig. 3 (c)). The periodic behavior of P and n are confirmed by the phase plane as shown in Fig. 3 (d). Therefore, the time series of P and n may be called periodic or regular pulse packages. For $f_m = 600\ MHz$, the time histories of P, n and $i(t)$ and phase plane are plotted in Fig. 4.

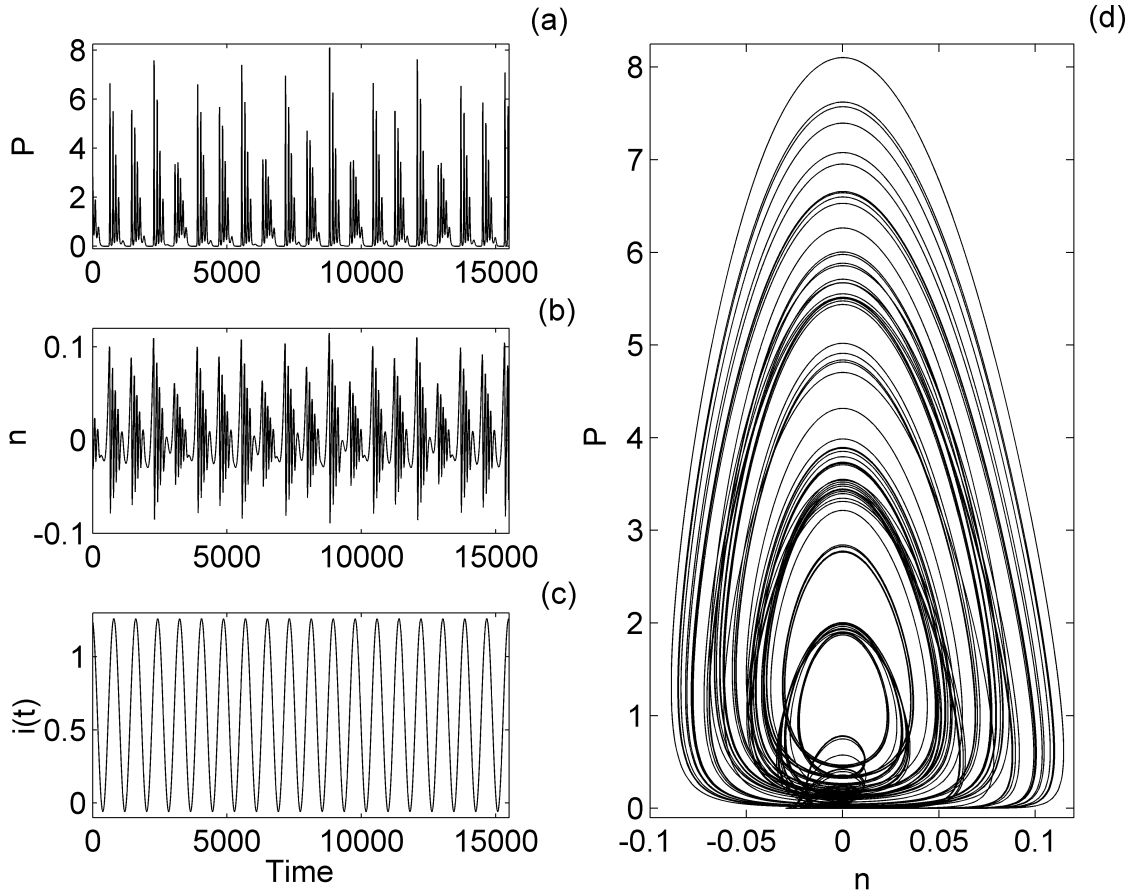

Figure 4: Time histories of P, n, $i(t)$ and phase plane for $f_m = 600\ MHz$. The others parameters are $i_{dc} = 0.6$ and $m = 1.1$. The initial conditions are ($P(0)$, $n(0)$) = (0.1, 0.001).

The photon density P and the carrier density n (see Figs. 4 (a) and (b)) alternate between a silent and an active phase. During the silent phase, the variables P and n have very small amplitudes, while the active phase is characterized by a sequence of pulses with decreasing amplitude and appeared in packages. Each package has its shape and appears irregularly. From the phase plane of Fig. 4 (d), one can see that the variables P and n exhibit chaotic pulse packages.

Microcontroller-based design scheme of single CMEESL is shown in Fig. 5.

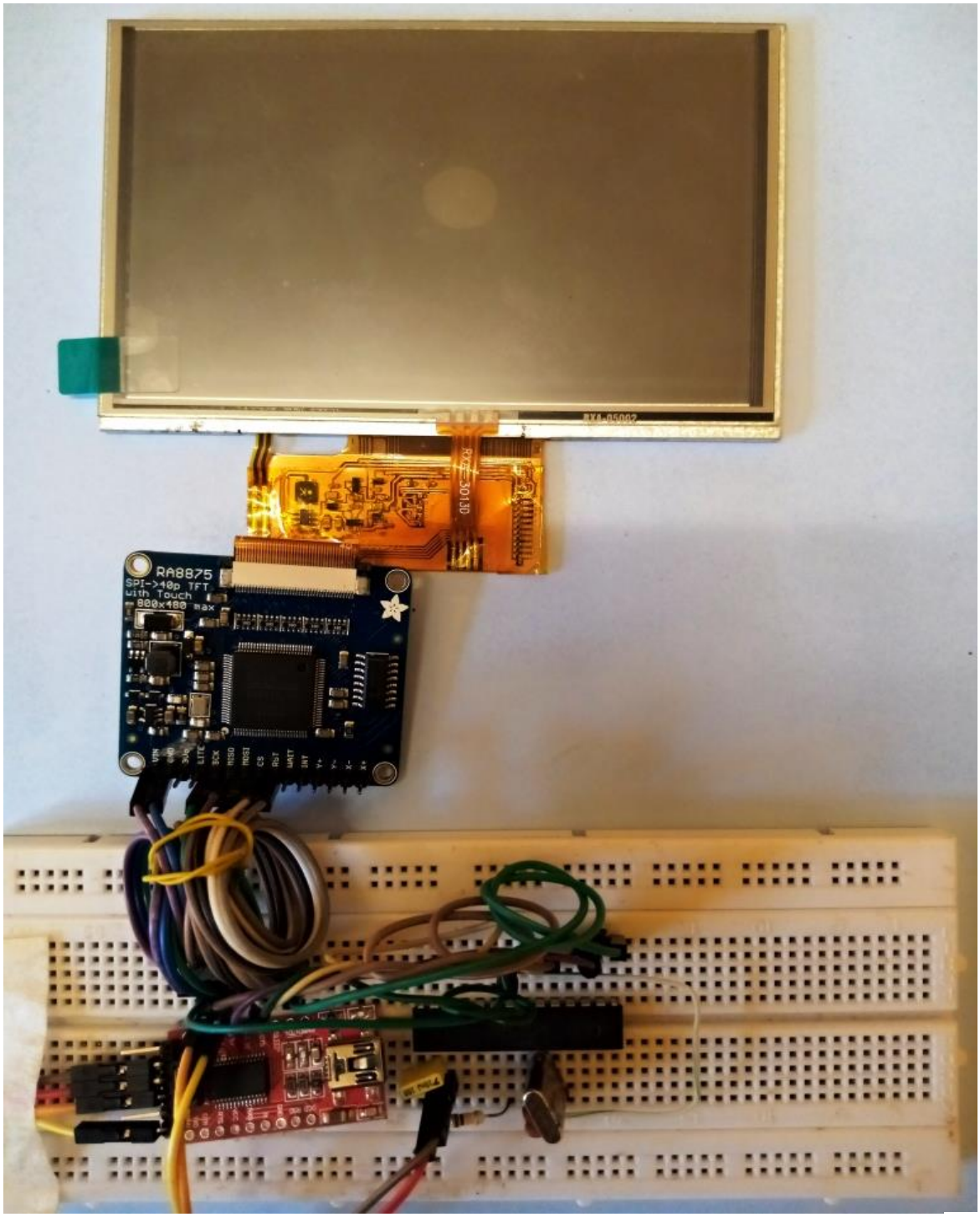

Figure 5: (Color online) Electronic circuit used for microcontroller implementation of single CMEESL.

The arithmetic and logic operations of Fig. 5 are implemented on the integrated circuit ATmega328P which is an 8-bit microcontroller based on the RISC architecture. This circuit has a

2 KB SRAM and a serial peripheral interface which is used by the microcontroller to communicate with the driver. The clock frequency is 16 MHz and the fourth order Runge-Kutta technique is the digital method used in this microcontroller. The FTD232 module is used for feeding the schematic and inserting the source code into ATmega328P. The visualization of phase portraits of microcontroller-based design scheme of single CMEESL presented in Fig. 6 is possible thanks to a TFT display of dimensions 800x480 connected to the microcontroller via the driver RA8875.

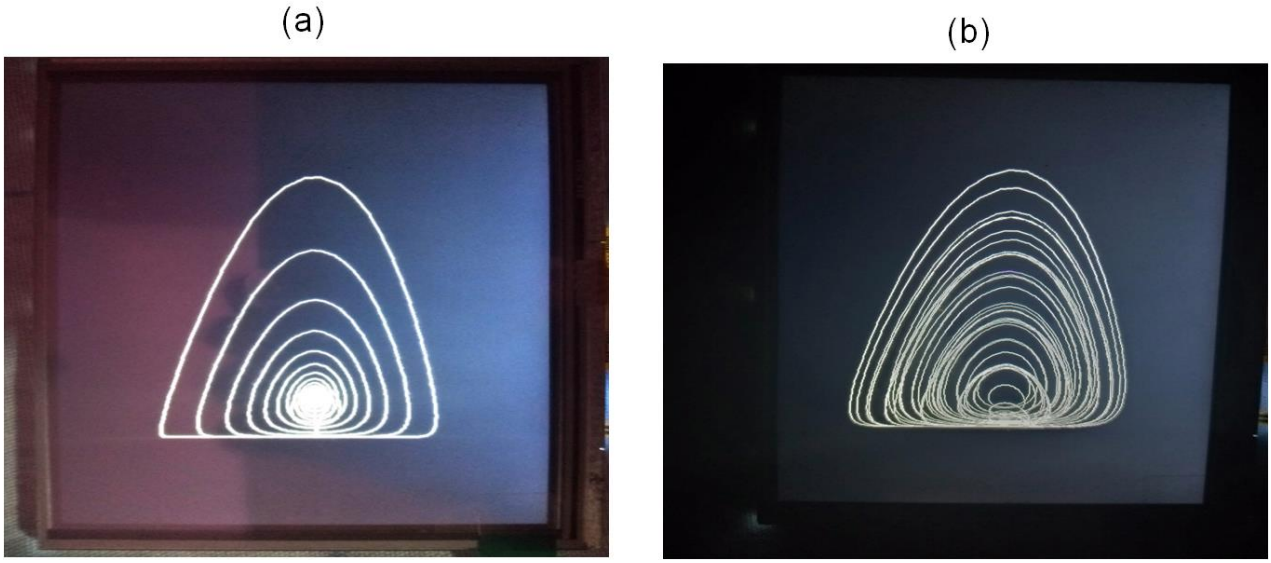

Figure 6: (Color online) Phase planes obtained from the microcontroller-based design scheme of single CMEESL in the plane $(n,\ P)$ illustrating (a) periodic and (b) chaotic pulses packages.

The good qualitative agreement between the microcontroller results of Fig. 6 and numerical simulations results of Figs. 3 (d) and 4 (d) confirms the existence of periodic and chaotic pulse packages found in single CMEESL.

III. Collective dynamics of CMEESLs in a lattice array

The investigation of single CMEESL is presented in the previous sections. Nonlinear coupled elements show the property of coherent synchronization to mention systems like neurons and semiconductor lasers **[23-27]**. When excited externally neurons show the properties of spiking, bursting and even chaos, which when compared to semiconductor lasers, similar properties like spiking and bursting oscillations are observed. This semiconductor lasers also show significant

characters like cluster synchronization and chimera states when considered in a lattice network of many coupled lasers. In **[23],** this semiconductor lasers subjected to optical feedback was used as a reservoir in the neural networks. In **[24]**, the authors discussed the synchronization phenomenon in a coupled laser network of 16 nodes. They were able to depict the dynamical behaviors of a network of lasers such as; cluster synchronization and anti-nodes but discussed little about chimera states. In this section, to analyze the network behavior of CMEESLs, a ring of nonlocally coupled 2N CMEESLs is considered whose inter coupling strength is defined by the parameter σ_e. Numerical simulations of the network, is base on the following mathematical model, defined as:

$$\frac{dP_i}{dt} = \left[(1+2n_i)(1-\sigma P_i)-1\right]P_i + \frac{\sigma_e}{2N}\sum_{j=i-N}^{i+N}\left(P_j - P_i\right), \tag{7a}$$

$$\frac{dn_i}{dt} = \varepsilon_0\left\{i_{dc}\left[1+ i_m \sin(\omega t)\right] - n_i - (1+2n)(1-\sigma P_i)P_i\right\}, \tag{7b}$$

where the values of parameters are identical to those used in Fig. 4 and the coupling strength σ_e is considered as the control parameter for this discussion. The term i denotes the number of lasers in the nodes and in this case is considered as $i = 1\ to\ 100$. The number of neighbors in the network is considered as N=10 and the snapshots are captured for 3000 s. The fourth order Runge-Kutta method **[28]** is used to numerically solve system (7) and the step size taken is h=0.005. The investigation starts by considering no coupling between the lasers in the lattice array as shown in Fig. 7 for $\sigma_e = 0$. As all the nodes are in random initial condition ($P_0 \in rand(0,0.1)$, $n_0 \in rand(0,1)$), the nodes are in their own state of oscillations and showing complete incoherency between them. This could be verified from the state plots shown in Fig. 7.

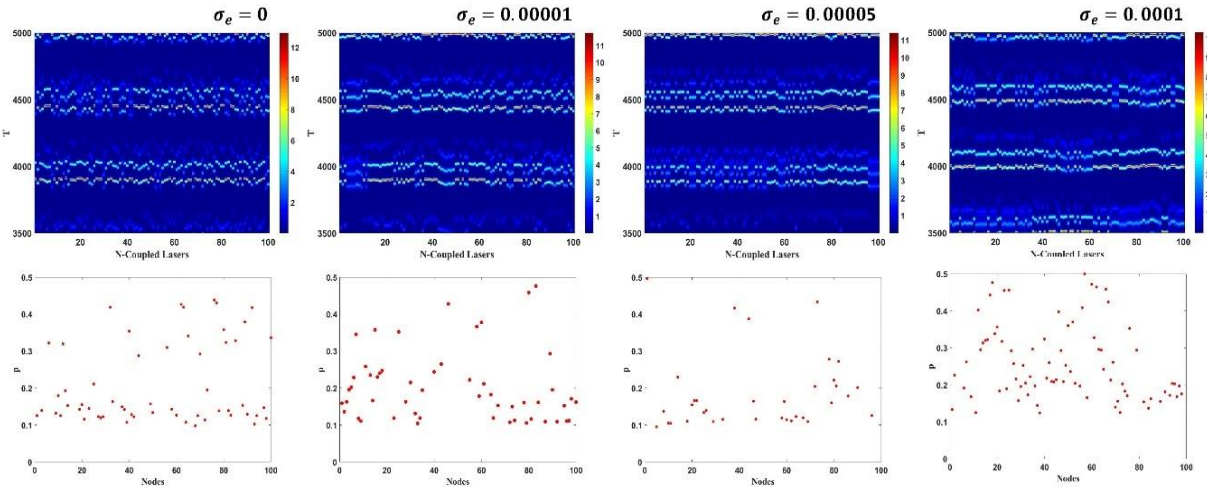

Figure 7: (Up) Snapshot of the network behavior of lasers defined by the model in system (7) and (Down) the corresponding state values of the nodes at the end of the simulation. Complete incoherency is observed in the figure for the selected coupling strengths.

A very small increase in the coupling strength as illustrated in Fig. 7 for $\sigma_g = 0.00001$, the network tries to achieve a cluster coherency but remains mostly incoherent. This scenario remains till $\sigma_g = 0.0001$ but as the coupling increases, the nodes tries to form a coherent pattern but later goes into incoherency because of the complex nonlinear character of the individual laser nodes. Reaching $\sigma_g = 0.0001$, the network shows asynchronous behavior. This is interesting to see the network performance for further increase in σ_g. By increasing the coupling strength to $\sigma_g = 0.0003$ as depicted in Fig. 8, it is observed that most nodes are in coherency while few nodes are still incoherent. This coexisting synchronous and asynchronous nodes in the network is termed as chimera **[25-27]**. Chimera state is a character shown by the network where the symmetry between the nodes is broken. These chimeras seen in neuronal networks are responsible for Parkinson's disease, epileptic seizures, and schizophrenia **[26]**. Such scenarios will result in disordered laser array with some lasers acting in complete incoherency resulting in loss of luminous power. Hence, this investigation is very important to know the ways of attaining complete synchrony in the lattice laser array.

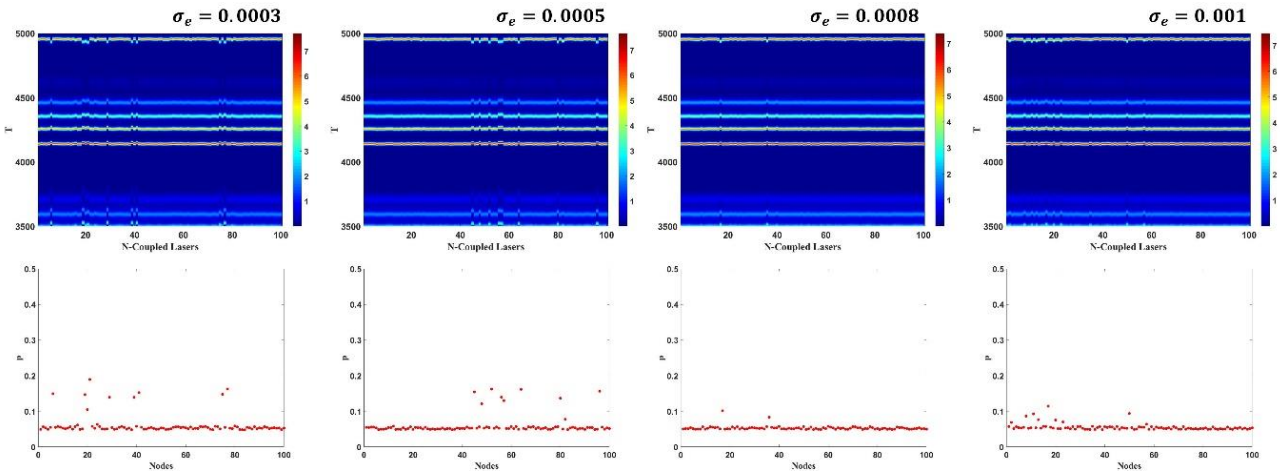

Figure 8: (Up) Snapshot of the network behavior of lasers defined by the model in system (7) and (Down) the corresponding state values of the nodes at the end of the simulation. The network shows chimera states and few nodes remain incoherent while most of the nodes enter coherency between them.

As shown in Fig. 8, chimera states exist from $\sigma_e = 0.0003$ to $\sigma_e = 0.001$. By increasing the coupling strength to $\sigma_e = 0.003$, asynchronous nodes drive towards synchronous nodes and further increase to $\sigma_e = 0.005$, the network is in complete coherency as illustrated in Fig. 9.

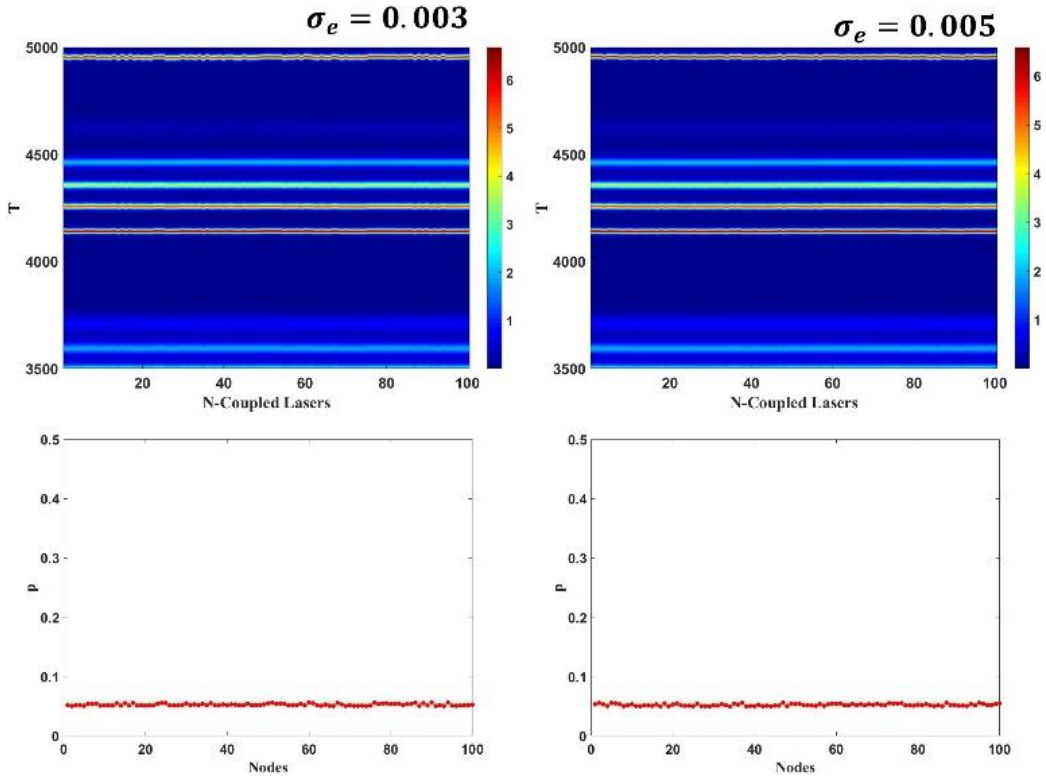

Figure 9: (Up) Snapshot of the network behavior of lasers defined by the model in system (7) and (Down) the corresponding state values of the nodes at the end of the simulation. The network that the node achieved complete coherency between them.

Thus in Fig. 9, chimera states are eliminated and such synchronous behaviors of the nodes increase the performance efficiency of CMEESLs array. The synchronous error between the nodes with their respective coupled nodes are calculated and presented in Fig. 10.

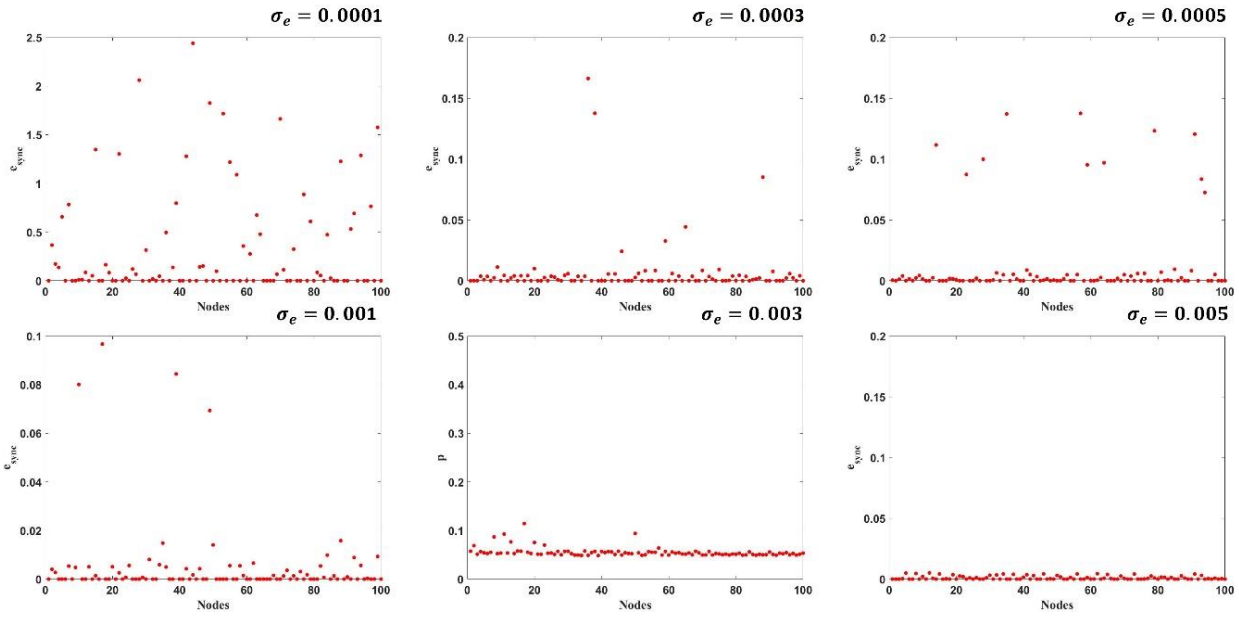

Figure 10: The synchronous errors between the nonlocally coupled nodes for various values of the coupling strength.

By comparing Fig. 10 with Figs. 7 to 9, it is noted that the asynchronous, chimera and synchronous behavior of the network can also be investigated using the synchronous error plots.

IV- Conclusion

This paper was devoted to the dynamical analysis of a single and network of current modulated edge emitting semiconductor lasers. Different dynamical behaviors of single current modulated edge emitting semiconductor laser including periodic and chaotic pulse packages were found using two- and one- dimensional parameter bifurcation diagrams. In order to access the physical feasibility of periodic and chaotic pulse packages found in single current modulated edge emitting semiconductor laser, its microcontroller circuit was implemented and validated on the integrated circuit ATMEGA328P microcontroller. The investigation of the network behavior of current modulated edge emitting semiconductor lasers revealed that by considering no coupling between the lasers in the lattice array, the nodes were in their own state of oscillations and showing complete incoherency between them. For very small increase in the coupling strength, the network was forced to achieve a cluster coherency but remains mostly incoherent. As the coupling strength increases, the nodes were forced to form a coherent pattern but they later returned to incoherency.

By increasing the coupling strength, the appearance of chimera states was observed, while further increasing the coupling strength, led to the elimination of chimera states and the network was in complete coherency.

Competing interests

The authors declare that they have no conflict of interest.

Funding Info

This work is partially funded by the Center for Nonlinear Systems, Chennai Institute of Technology, India via funding number CIT/CNS/2021/RD/064.

Author contributions

Dhanagopal Ramachandran and Nasr Saeed developed the model and theoretically analyzed the rate-equations of the proposed model. André Rodrigue Tchamda and Sifeu Takougang Kingni did the microcontroller implementation of the proposed model. Dhanagopal Ramachandran and Anitha Karthikeyan did the dynamical analysis of the proposed model in a lattice array. Nasr Saeed and Iqtadar Hussain participated in the data analysis at different stages. All authors contributed to the interpretation of the results and writing of the manuscript.

Consent to Participate (Ethics)

Not applicable

Consent to Publish (Ethics)

Not applicable

References

[1] T. H. Maiman, Stimulated optical radiation in ruby, Nature 187, 493-494 (1960).

[2] T. L. Koch and U. Koren, Semiconductor lasers for coherent optical fiber communications, Lightwave Technology Journal 8, 274-293 (1990).

[3] W. W. Chow and S. W. Koch, Semiconductor-Laser Fundamentals, Springer, Berlin (1999).

[4] J. V. Moloney, J. Hader and S.W. Koch, Quantum design of semiconductor active materials: laser and amplifier applications, Laser & Photon. Rev. 1, 24-43 (2007).

[5] G. Verschaffelt, M. Khoder and G. Van der Sande, Random number generator based on an integrated laser with on-chip optical feedback, Chaos 27, 114310-114316 (2017) .

[6] D. Rontani, D. Choi, C.-Y. Chang, A Locquet and D.S. Citrin, Compressive sensing with optical chaos, Sci. Rep. 6, 35206-35212 (2016).

[7] J.-P. Goedgebuer, L. Larger, H. Porte, Optical cryptosystem based on synchronization of hyperchaos generated by a delayed feedback tunable laser diode, Phys. Rev. Lett. 80, 2249–2252 (1998).

[8] A. Argyris, D. Syvridis, L. Larger, V. Annovazzi-Lodi P. Colet, I. Fischer, J. García-Ojalvo, C.R. Mirasso, L. Pesquera, K.A Shore, Chaos-based communications at high bit rates using commercial fibre-optic links, Nature (London, U.K.) 437, 343–346 (2005).

[9] J.-G. Wu, Z.-M. Wu, G.-Q. Xia, T. Deng, X.-D. Lin, X. Tang, G.-Y. Feng, Isochronous synchronization between chaotic semiconductor lasers over 40-km fiber links, IEEE Photonics Technol. Lett. 23, 1854–1856 (2011).

[10] P. Li, J.-G. Wu, Z.-M. Wu, X.-D. Lin, D. Deng, Y.-R. Liu, G.-Q. Xia, Bidirectional chaos communication between two outer semiconductor lasers coupled mutually with a central semiconductor laser, Opt. Express 24, 23921–23931 (2011).

[11] J.-G. Wu, Z.-M. Wu, X. Tang, L. Fan, W. Deng, G.-Q. Xia, Experimental Demonstration of LD-Based Bidirectional Fiber-Optic Chaos Communication, IEEE Photonics Technol. Lett. 25, 587–590 (2013).

[12] Z. Cao, L. Zou, L. Chen, J. Yu, Impairment mitigation for a 60 GHz OFDM radio-over-fiber system through an adaptive modulation technique, J. Opt. Commun. Networks 3, 758–766 (2011).

[13] S. T. Kingni, G. Van der Sande, L. Gelens, T. Erneux and J. Danckaert, Direct modulation of semiconductor ring lasers: Numerical and asymptotic analysis, JOSA B 29, 1983–1992 (2012).

[14] M. Sciamanna, A. Valle, P. Megret, M. Blondel, K. Panajotov, Nonlinear polarization dynamics in directly modulated vertical-cavity surface-emitting lasers, Phys. Rev. E 68, 016207-016210 (2003).

[15] C. Masoller, M.S. Torre, K.A. Shore, Polarization dynamics of current modulated vertical-cavity surface-emitting lasers, IEEE J. Quantum Electron. 43, 1074-1082 (2007).

[16] A. Valle, M. Sciamanna, K. Panajotov, Nonlinear dynamics of the polarization of multitransverse mode vertical-cavity surface-emitting lasers under current modulation, Phys. Rev. E 76, 046206-046214 (2007).

[17] J.H. Talla Mbe, K.S. Takougang and P. Woafo, Chaos and pulse packages in current-modulated vertical cavity surface-emitting lasers, Phys. Scr. 81, 035002-035010 (2010).

[18] S. T. Kingni, J. H. Talla Mbé, P. Woafo, Nonlinear dynamics in VCSELs driven by a sinusoidally modulated current and Rossler oscillator, Eur. Phys. J. Plus 127, 46–55 (2012).

[19] Y. Chembo, P. Woafo, Stability analysis for the synchronization of semiconductor lasers with ultra-high frequency current modulation. Phys. Lett. A 308, 381–390 (2003).

[20] T. Heil, I. Fischer, W. Elsäßer and A. Gavrielides, Dynamics of semiconductor lasers subject to delayed optical feedback: The short cavity regime. Phys. Rev. Lett. 87, 243901-243904 (2001).

[21] A. Tabaka, M. Peil, M. Sciamanna, I. Fischer, W. Elsäßer, H. Thienpont, I. Veretennicoff and K. Panajotov, Dynamics of vertical-cavity surface-emitting lasers in the short external cavity regime: Pulse packages and polarization mode competition, Phys. Rev. A 73, 013810-013823 (2006).

[22] A. Takeda, R. Shogenji and J. Ohtsubo, Dynamics and pulse-package oscillations in broad-area semiconductor lasers with short optical feedback, Appl. Phys. Lett. 101, 231105-231107 (2012).

[23] J. Ohtsubo, Semiconductor Laser Networks: Synchrony, Consistency, and Analogy of Synaptic Neurons. In: Semiconductor Lasers. Springer Series in Optical Sciences, vol 111. Springer, Cham., 559-596 (2017).

[24] A. Argyris, M. Bourmpos, and D. Syvridis, Experimental synchrony of semiconductor lasers in coupled networks, Opt. Express 24, 5600-5614 (2016).

[25] D. Dudkowski, Y. Maistrenko and T. Kapitaniak, Different types of chimera states: An interplay between spatial and dynamical chaos, Phys. Rev. E 90, 032920-032924 (2014).

[26] S. Majhi, B. K. Bera, D. Ghosh, M. Perc, Chimera states in neuronal networks: A review, Physics of Life Reviews 28, 100-121 (2019).

[27] S. Wang, S. He, K. Rajagopal, A. Karthikeyan and K. Sun, Route to hyperchaos and chimera states in a network of modified Hindmarsh-Rose neuron model with electromagnetic flux and external excitation, Eur. Phys. J. Spec. Top. 229, 929–942 (2020).

[28] W. H. Press, S. A. Teukolsky, W .T. Vetterling and B. P. Flannery, Numerical Recipes: The Art of Scientific Computing, Cambridge University Press, N.Y., (2007).